Biochemical Characterization of the Histidine Triad Protein PhtD as a Cell Surface Zinc-Binding Protein of Pneumococcus

9 AUTHORS, INCLUDING:

Anne Imberty
French National Centre for Scientific Research
361 PUBLICATIONS **10,380** CITATIONS

SEE PROFILE

Benoit Gallet
Institut de Biologie Structurale (IBS), Grenob…
10 PUBLICATIONS **93** CITATIONS

SEE PROFILE

Annemarie Diguilmi
Institut de Biologie Structurale (IBS)
39 PUBLICATIONS **980** CITATIONS

SEE PROFILE

Jeremy S Brown
University College London
109 PUBLICATIONS **1,775** CITATIONS

SEE PROFILE

Biochemical Characterization of the Histidine Triad Protein PhtD as a Cell Surface Zinc-Binding Protein of Pneumococcus

Elodie Loisel,[†] Suneeta Chimalapati,[‡] Catherine Bougault,[†] Anne Imberty,[§] Benoit Gallet,[†] Anne Marie Di Guilmi,[†] Jeremy Brown,[‡] Thierry Vernet,[*,†] and Claire Durmort[†]

[†]CEA, Institut de Biologie Structurale Jean-Pierre Ebel, Grenoble, France, CNRS, Institut de Biologie Structurale Jean-Pierre Ebel, Grenoble, France, and Université Joseph Fourier-Grenoble 1, Institut de Biologie Structurale Jean-Pierre Ebel, Grenoble, France

[‡]Centre for Respiratory Research, Department of Medicine, Royal Free and University College Medical School, London WC1E 6JF, United Kingdom

[§]CERMAV-CNRS (affiliated with Université Joseph Fourier and ICMG), 601 rue de la Chimie, BP53, 38041 Grenoble cedex 09, France

ABSTRACT: Zinc homeostasis is critical for pathogen host colonization. Indeed, during invasion, *Streptococcus pneumoniae* has to finely regulate zinc transport to cope with a wide range of Zn^{2+} concentrations within the various host niches. AdcAII was identified as a pneumococcal Zn^{2+}-binding protein; its gene is present in an operon together with the *phtD* gene. PhtD belongs to the histidine triad protein family, but to date, its function has not been clarified. Using several complementary biochemical methods, we provide evidence that like AdcAII, PhtD is a metal-binding protein specific for zinc. When Zn^{2+} binds ($K_d = 131 \pm 10$ nM), the protein displays substantial thermal stabilization. We also present the first direct evidence of a joint function of AdcAII and PhtD by demonstrating that their expression is corepressed by Zn^{2+}, that they interact directly in vitro, and that they are colocalized at the bacterial surface. These results suggest the common involvement of the AdcAII−PhtD system in pneumococcal zinc homeostasis.
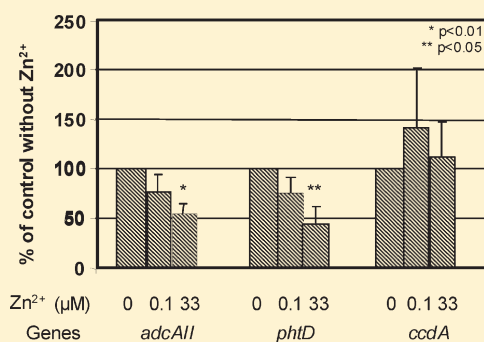
*S*treptococcus pneumoniae asymptomatically colonizes the human nasopharynx but also crosses tissue barriers to cause lower-respiratory tract infections as well as septicaemia and meningitis. During invasive infection, pathogenic bacteria have to deal with fluctuating Zn^{2+} concentrations encountered in the various host niches. This metal can be rare in certain host compartments (10^{-4} μM labile Zn^{2+} in blood plasma[1]) and abundant in others, including human bronchial epithelium where Zn^{2+} accumulates at the apical cell surface.[2] Although Zn^{2+} is a vital trace element to the bacterium, this metal is toxic at high concentrations, as it competes with other metal ions for binding to the active site of enzymes. As a consequence, to survive these drastic changes in metal abundance, bacteria must possess efficient metal homeostasis mechanisms. Proteins involved in Zn^{2+} efflux or uptake systems may thus promote bacterial fitness during infection and affect virulence.

AdcAII has been previously described as a Zn^{2+}-binding protein homologous to metal-binding receptors (MBRs).[3] Recent studies point toward a role of the homologous laminin-binding protein (Lsp or Lbp) from *Streptococcus pyogenes* in Zn^{2+} homeostasis and virulence.[4,5] Deletion of the *lsp* gene in *S. pyogenes* markedly reduces bacterial virulence in murine models of subcutaneous infection.[4,5] However, the genomic organization of the corresponding genes, *lsp* from *S. pyogenes* and *adcAII* (also called *lmb*; *spr0906* in the R6 pneumococcus strain), is different from that of the classical MBR genes that usually belong to an operon including genes for a permease, an ATPase, and a regulator. In contrast, the *adcAII* gene belongs to a transcript encompassing five genes from *ccdA* to *phtD*

where *adcaII* and *phtD* are contiguous (Figure 1A).[3] The protein AdcR has been shown to be a Zn^{2+}-dependent transcriptional repressor, and two adjacent repeats of imperfect AdcR-binding palindromes were identified upstream of the *adcAII* gene, suggesting AdcR can regulate expression of *adcaII* and *pht*. Indeed, overexpression of these genes has been recently identified using a comparative DNA microarray analysis of isogenic wild-type and Δ*adcR* pneumococcus strains.[6] Taken together, these data suggest a transcriptional coregulation of *adcAII* and *phtD* genes that implies a functional link between both proteins.

PhtD is a surface protein[7−9] that belongs to the histidine triad protein (Pht) family, characterized by the presence of four to six histidine triad motifs (HxxHxH) that frequently bind divalent metal cations.[10] The crystal structure of a short fragment of PhtA containing one HxxHxH motif has been determined in complex with Zn^{2+}, suggesting Pht proteins do bind divalent cations, but their metal specificity remains to be established.[11,12] Despite the promising use of Pht proteins in recent protein vaccine developments,[13] their structure and function remain unknown.

In this study, we ascertain that, like AdcAII, the PhtD protein specifically binds Zn^{2+} in vitro. We provide evidence that the expression of both proteins is coregulated by Zn^{2+} and that they interact with each other in vitro. Both proteins are colocalized at
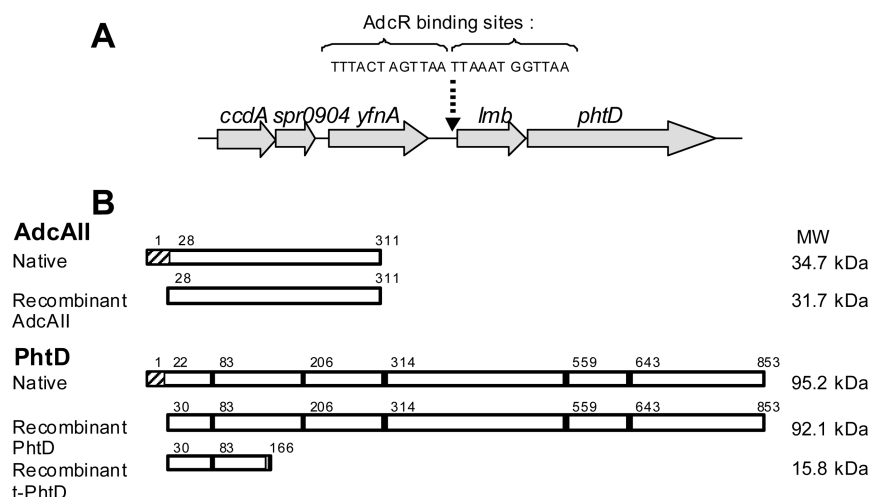
Figure 1. Topology of the *adcAII*- and *phtD*-containing operon and these recombinant proteins. (A) Genetic organization of the operon containing the *lmb* (*adcAII*) and *phtD* genes. The localization and the sequence of the two AdcR binding sites are indicated. (B) Schematic representation of the native forms and the recombinant constructs of AdcAII and PhtD proteins drawn to scale. The signal peptides of the native proteins are indicated by hatched boxes. HxxHxH motifs are represented by black boxes, with numbers indicating the position of the first His residue of the motif. The C-terminal SHNHNS sequence of t-PhtD is colored gray.

the cell surface, anchored via two different systems. Indeed, we prove that AdcAII is a lipoprotein that is bound to membrane phospholipids whereas PhtD is mainly embedded in the cell wall.

■ EXPERIMENTAL PROCEDURES

Bacterial Strains and Growth Conditions. Strain D39 is an encapsulated strain from serotype 2, and strain R6 is a none-ncapsulated derivative of D39 (Rockefeller University, New York, NY). Cells were grown at 37 °C in an atmosphere of 95% air and 5% CO_2 in Bacto Todd Hewitt Broth (TH broth) (Difco) or in a chemically defined medium (CDM)[14] supplemented with 5 mg/L choline but without L-asparagine, L-cystine, hydroxy-L-proline, and L-tyrosine. The construction of the Δlsp mutant has been described previously.[15] Briefly, the *lsp* deletion mutant was obtained by transformation of the wild-type D39 strain with a polymerase chain reaction (PCR) product containing the *erm* cassette from pACH74 to replace the *lsp* gene.

Q-PCR Experiments. Pellets of *S. pneumoniae* R6 cells cultured in CDM containing different Zn^{2+} concentrations were treated with 15 mg/mL lysozyme in PBS for 10 min at room temperature. Then, 25 mg of acidic washed glass beads (Sigma) was added, and cells were disrupted by vigorous vortexing for 10 min. RNAs were purified from the supernatant according to the Macherey Nucleospin RNAII kit instructions. RNA quantity and quality were determined by measurement of the ratios of absorbance at 260 and 280 nm. RNA samples were subjected to PCR amplification to ensure the absence of contaminating chromosomal DNA. cDNA conversion was performed in 50 μL reaction mixtures via combination of 5 μg of total RNA and 100 ng of random hexamers using the Superscript First-Strand Synthesis kit (Invitrogen). Aliquots of 2.5 μL of cDNA were used as templates for Q-PCR experiments [IQ5 96-well format real-time PCR instrument (Bio-Rad)] using the required primers at 0.3 μM and 10 μL of a mix for real-time PCR (iQ SYBR^R Green Supermix, Bio-Rad). The following primer pairs were used: gctgccataccaaggtgaag and ggttgtctctcgtatcgttcc for *rpoB*, aaggaaagtcagacaggaaaggg and tgccgaaggttcaaaggagtg for *adcAII*, acctgcaccaaatcctcaac and tttgctatcaatgcctgctg for *phtD*,

tttccaacatccctttccttg and gcggaaaatcagcatgaaat for *adcR*, gggtcttcacca-gatggaaa and gaagccgcaagtgctaaaac for *ccdA*, and caacatttcttgggcgattt and gtgcgtttcctctttgaagc for *adcA*. *rpoB* was used as an internal control. For each primer pair, standard quantitative curves were generated from serial dilutions of PCR products and were utilized for a quantitative analysis of the gene of interest. Target gene transcription levels were expressed as a percentage of the control that corresponds to *S. pneumoniae* cultured in CDM without addition of Zn^{2+}. Each sample was analyzed twice. Data reported represent the mean and standard deviation derived from at least four independent experiments.

Protein Expression. Pellets of *S. pneumoniae* R6 cells cultured in CDM containing different Zn^{2+} concentrations were resuspended in water. Equal amounts of total bacterial lysates were submitted to 12.5% sodium dodecyl sulfate—polyacrylamide gel electrophoresis (SDS—PAGE), immunoblotted using specific antibodies, and revealed by chemiluminescence detection with the ECL system (GE Healthcare). Protein amounts were quantified using the Molecular Imager Gel Doc XR system and Quantity One (Bio-Rad). Enolase was used as an internal standard for housekeeping protein expression.

Construction of PhtD and t-PhtD Plasmids for Recombinant Expression. DNA from the R6 strain of *S. pneumoniae* was used as a template to PCR-amplify the sequence of the *phtD* gene using the Phusion polymerase. The primers were designed to remove the N-terminal signal peptide and the LxxC motif (residues 1—29). The PCR product was cloned into pLIM09 vector (RobioMol, Grenoble, France). The resulting pLIM09-*phtD* plasmid allows expression of the PhtD protein from Gly30 to Glu853 fused to a His$_6$ tag at the N-terminus. A tobacco etch virus (TEV) protease cleavable site (ENLYFQG) was inserted between the His$_6$ tag and the N-terminal sequence of PhtD (Figure 1B). A truncated form of PhtD (t-PhtD) was constructed by mutating AGA codon 167 in pLIM09-*phtD* into a TGA stop codon allowing expression of PhtD, from Gly30 to Ser166 (Figure 1B).

Production and Purification of Recombinant Proteins. Recombinant AdcAII was expressed and purified onto a NiN-TA-agarose column (Qiagen) as previously described.[3] PhtD and

t-PhtD expression and purification follow a similar protocol. Briefly, *Escherichia coli* strain BL21(DE3)RIL harboring the corresponding plasmids was grown in Terrific Broth supplemented with 30 μg/mL kanamycin at 37 °C until the OD_{600} reached 0.8. Expression was induced with 0.5 mM isopropyl β-D-1-thiogalactopyranoside (IPTG) overnight at 27 °C. After cell disruption, the soluble recombinant proteins were purified on a NiNTA-agarose column according to the manufacturer's instructions. PhtD protein was submitted to a second gel filtration chromatography purification step using a Superdex 200 prep grade (GE Healthcare) column. After cleavage of the His_6 tag with the TEV protease, both PhtD and t-PhtD proteins were concentrated and dialyzed against a 50 mM HEPES (pH 8), 50 mM NaCl buffer. ICP-MS analyses were performed by the Service Central d'Analyze in Lyon, France, on 7.9 mg/mL PhtD and 3.0 mg/mL t-PhtD proteins. The dialysis buffer was used as a blank.

To generate the apo forms of AdcAII, PhtD, and t-PhtD, the proteins were extensively dialyzed against 50 mM HEPES (pH 8), 50 mM NaCl, and 10 mM EDTA. EDTA was then removed by dialysis in the presence of Chelex 100 resin (Bio-Rad) to remove any trace of metal ion in the buffer. All subsequent experiments involving the apoproteins were conducted in buffers previously treated with the Chelex 100 resin.

Thermal Shift Assay (TSA). TSA experiments with PhtD were conducted using an IQ5 96-well format real-time PCR instrument (Bio-Rad) as previously described.[16] Briefly, 6 μM recombinant apo-PhtD protein was mixed with 2 μL of 500× Sypro Orange (Molecular Probes) diluted (1:5) in water with or without 120 μM metal salts. Samples were heat-denatured from 20 to 100 °C at a rate of 1 °C/min. Protein thermal unfolding curves were monitored by detection of changes in the fluorescence of the Sypro Orange. The inflection point of the fluorescence versus temperature was identified by plotting the first derivative. The minima of the derivative were termed the melting temperatures (T_m). The fluorescence values of buffers and salt solutions were checked as controls.

Isothermal Titration Calorimetry (ITC). ITC experiments were conducted with a VP-ITC isothermal titration calorimeter (Microcal) at 25 °C. Protein and metal salts were dissolved in identical buffer, i.e., 50 mM MES (pH 6.3) and 50 mM NaCl. The protein concentration in the microcalorimeter cell was set to approximately 10 μM. Protein concentrations were precisely determined by spectrophotometry at 280 nm ($\varepsilon = 14729$ mol^{-1} L cm^{-1}, as determined through amino acid analysis) using a Nanodrop spectrophotometer (ND-1000, Isogen Life Science). A total of 30 serial injections of 6 μL of 120 μM salt solutions were performed at a stirring speed of 450 rpm with an injection spacing of 5 min. To correct the experimental binding isotherm for background heat effects, salt containing buffers was titrated into buffer, buffer was titrated into the protein solution, and the corresponding heat changes were recorded. The experimental data were fitted to a theoretical titration curve using the one-set-of-sites fitting model provided with the Microcal data analysis software.

Cross-Linking Experiments. Recombinant AdcAII (146 μM) was mixed with either PhtD or t-PhtD at 18.4 μM. The mixture was incubated for 1 h at room temperature, followed by 15 min incubation in the presence of 0.5 mM bis(sulfosuccinimidyl) suberate (BS3) (Sigma-Aldrich). BS3 was then inactivated with 25 mM Tris (pH 8) for 15 min before samples (3 μL each) were loaded on a SDS—PAGE gel to be analyzed by Western blotting. Immunodetection of AdcAII was performed first. The nitrocellulose membrane was then stripped for 15 min at 50 °C in 60 mM Tris (pH 6.8), 100 mM β-mercaptoethanol, and 2% sodium

dodecyl sulfate (SDS). The disappearance of the AdcAII signal was checked before the second revelation was performed with an antibody against PhtD. The whole experiment was repeated three times, with two independent batches of recombinant proteins.

Membrane Protein Extraction and Subcellular Fractionation. Bacteria were grown to late exponential phase in TH broth. Membrane proteins were extracted with Triton TX114 as described previously.[17,18] Briefly, exponentially growing bacteria were pelleted and incubated with 1% deoxycholic acid in PBS at 37 °C for 30 min and were further lysed by ultrasonication. The lysates were incubated with 800 μL of PBS and 100 μL of 10% Triton TX114 at 4 °C for 2 h, followed by centrifugation to pellet debris. The supernatants were then incubated at 37 °C to allow phase separation followed by centrifugation at room temperature to pellet the detergent soluble proteins. These detergent soluble membrane proteins were then washed with PBS followed by incubation at 37 °C and centrifugation to pellet the proteins. The membrane proteins were diluted 1:4 in PBS prior to SDS—PAGE using the appropriate acrylamide concentration (10 or 15%).

For subcellular fractionation, cells were disrupted via a 90 min incubation in 50 mM HEPES (pH 8), 50 mM NaCl, 1 mM PMSF, complete EDTA-free (Roche Diagnostics), 100 μg/mL lysozyme, 20 units/mL mutanolysine, 1 unit/mL DNase, and 2 mM MgCl$_2$ followed by ultrasonic lysis. A first centrifugation for 15 min at 3000 g segregated the soluble cytoplasmic compartment from the cell wall fraction. This soluble supernatant was subjected to a 16 h ultracentrifugation at 180000 g to separate the cytosol from the membrane-containing fraction. An equivalent amount of each fraction was loaded on a 12.5% SDS—PAGE gel for subsequent immunoblotting.

Immunofluorescence Microscopy and Colocalization. The immunostaining protocol of *S. pneumoniae* R6 cells was adapted from that of Harry et al.[19] Briefly, bacteria grown at an OD_{600} of 0.3 in TH broth were fixed with 4% paraformaldehyde for 20 min in ice. Cells were then deposited onto poly-L-lysine-coated Poly Prep slides (Sigma-Aldrich) and permeabilized in cold methanol for 5 min. Slides were blocked for 30 min at room temperature with 5% (w/v) nonfat dry milk in PBS (saturation buffer) and then incubated for 1 h with appropriate dilutions of anti-AdcAII and/or anti-PhtD antibodies in saturation buffer. The slides were then washed twice in PBS and incubated with a 1:300 dilution of Cy3-conjugated goat anti-rabbit and/or Cy2-conjugated goat anti-mouse immunoglobulin G (Jackson Immunoresearch) in saturation buffer. After successive washes with PBS and water, cells were incubated with 2 μg/mL 6-diamidino-2-phenylindole (DAPI) (TEBU) for 15 min. Slides were mounted with moviol and examined with an Olympus BX61 microscope equipped with an UPFLN 100× O-2PH/1.3 objective and a QImaging Retiga-SRV 1394 cooled charge-coupled device camera. Image acquisition was performed using Volocity without any further picture processing.

■ RESULTS

PhtD Is a Zn^{2+}-Binding Protein. We previously showed that AdcAII is a Zn^{2+}-binding protein and that *adcAII* (also known as *lmb*) and *phtD* genes are cotranscribed in an operon downstream of two adjacent AdcR-binding sites, a Zn^{2+}-dependent transcriptional repressor (Figure 1A).[3] The putative ability of PhtD to bind zinc is based on the presence of five histidine triads in its sequence, as depicted in Figure 1B. To validate this hypothesis, we produced
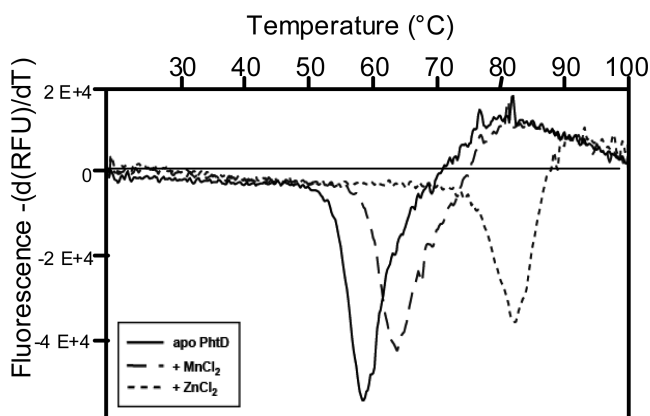
Figure 2. Thermal stability of the PhtD protein. Thermal unfolding of 6 μM Apo-PhtD was followed in the presence of the Sypro Orange fluorescent probe in the absence or presence of 1 equiv of $MnCl_2$ or $ZnCl_2$. The samples were heated from 20 to 95 °C at a heating rate of 1 °C/min. The plot of the first derivative of the fluorescence intensity vs the temperature $[-d(RFU)/dT]$ allows accurate determination of the minima that give the melting temperatures (T_m). This set of curves is representative of three independent experiments.

the full-length recombinant PhtD protein (amino acids 30−853) in *E. coli* for subsequent ICP-MS analysis directly after protein purification. Zn^{2+} was identified in PhtD samples at a molar ion: protein ratio of 4.6 ± 0.1. Ni^{2+} was also found at a molar ion: protein ratio of 0.5 ± 0.1. The presence of nickel probably originates from the Ni^{2+} affinity purification step. Therefore, recombinant PhtD is a Zn^{2+}-binding protein that most likely possesses five metal binding sites. As the full-length recombinant PhtD protein was highly susceptible to protease degradation during the purification steps, we also cloned and purified a stable 16 kDa truncated fragment of the protein called t-PhtD [amino acids 30−166 (Figure 1B)]. t-PhtD has one histidine triad (HxxHxH) and was found to contain 1.6 ± 0.1 zinc atoms per protein using ICP-MS analysis. The exposed C-terminal polyhistidine motif (SHNHNS), present only in t-PhtD, is likely to bind zinc, causing the molar ion:protein ratio to be greater than 1.

To ensure that zinc binding is not an artifact due to the production of the recombinant protein in the Zn^{2+}-rich cytoplasm of *E. coli*, in vitro experiments were conducted to compare the behavior of apo-PhtD with that of the protein bound to two different physiologically abundant metal ions (Zn^{2+} and Mn^{2+}). Because binding a specific metal generally stabilizes proteins, we used the thermal shift assay (TSA) to compare the impact of these metals on PhtD stability. The recombinant PhtD and t-PhtD proteins were gradually heated, and the unfolding process was monitored with Sypro Orange as a fluorescent probe. For each condition, the first derivative of the fluorescence intensity versus the temperature was plotted to determine the T_m value. Unfortunately, t-PhtD did not generate any TSA signal, probably as a consequence of its predicted β-sheet conformation. However, full-length PhtD gave a high-intensity fluorescent signal allowing TSA to be assessed. As shown in Figure 2, the apo form of PhtD has a T_m of 59.4 ± 0.2 °C. In the presence of Mn^{2+} ions, the T_m increases slightly to 65.6 ± 1.1 °C. Under identical experimental conditions, the addition of Zn^{2+} ions triggers a marked increase in protein stability, leading to a T_m of 82.3 ± 0.6 °C. T_m shifts induced by Mn^{2+} and Zn^{2+} were totally reversible when EDTA was added in excess (data not shown).
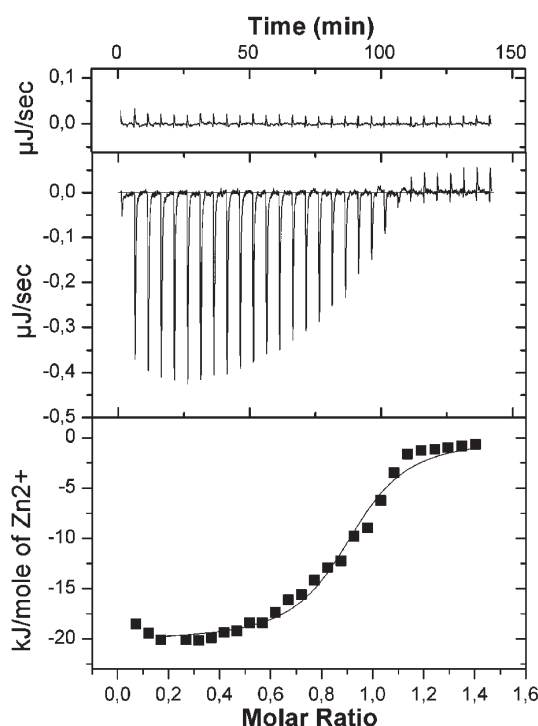

Figure 3. Titration microcalorimetry data of t-PhtD with Zn^{2+} and Mn^{2+}. Thirty 6 μL automatic injections of a 120 μM salt solution were performed in 10 μM t-PhtD placed in the cell at 25 °C. The heat released per mole of titrant as a function of the molar ratio of total ligand to total protein was obtained from the titration and fitted to a single-site binding equation: $MnCl_2$ (top) and $ZnCl_2$ (middle and bottom).

The large stabilizing effect of Zn^{2+} on PthD for a 1:1 molar ratio suggests a high affinity for this metal.

t-PhtD Binds Zn^{2+} with a Nanomolar Affinity. The affinity of the interaction of Zn^{2+} with t-PhtD was measured by microcalorimetry. The heat evolved per mole of titrant as a function of the molar ratio of total ligand to total protein was obtained from thermograms for t-PhtD titrated with $ZnCl_2$. The interaction was exothermic with a stoichiometry close to one. The data could be fitted to a single-site binding equation (Figure 3) giving a stoichiometry value of 0.88 and an association constant of $(7.8 ± 0.6) \times 10^6\ M^{-1}$ ($K_d = 131 ± 10$ nM), confirming the presence of one single high-affinity Zn^{2+} binding site in the t-PhtD fragment. The thermodynamic parameters derived indicate almost equivalent favorable participation of the enthalpic contribution ($\Delta H = -19 ± 0.2$ kJ mol^{-1}) and the entropic term ($T\Delta S = 19 ± 0.4$ kJ mol^{-1}). Enthalpic values show significant similarity with data [$\Delta H = -26.8 ± 1.2$ kJ mol^{-1} in 10 mM ACES buffer (pH 7) at 25 °C] for carbonic anhydrase, a protein that exhibits a $His_3(H_2O)$ Zn(II) coordination site ($H^{94}XH^{96}X_{22}H^{119}$), and marked differences [$\Delta H = -81.1 ± 2.5$ kJ mol^{-1} in MES buffer (pH 6) at 25 °C] with zinc finger proteins with Cys_2His_2 coordination sites.[20] The thermodynamic results are thus consistent with Zn^{2+} binding by the histidine triad. The titration of t-PhtD with Mn^{2+} metal was also determined for the same ligand and protein concentrations. As shown in Figure 3 (top panel), Mn^{2+} did not interact with tPhtD and had no enthalpic signature.

AdcAII and PhtD Interact in Vitro. As we have shown that AdcAII and PhtD proteins are both Zn^{2+}-binding proteins and that *adcAII* and *phtD* genes are cotranscribed in a single operon (Figure 1A), we wondered if these proteins belonged to the same
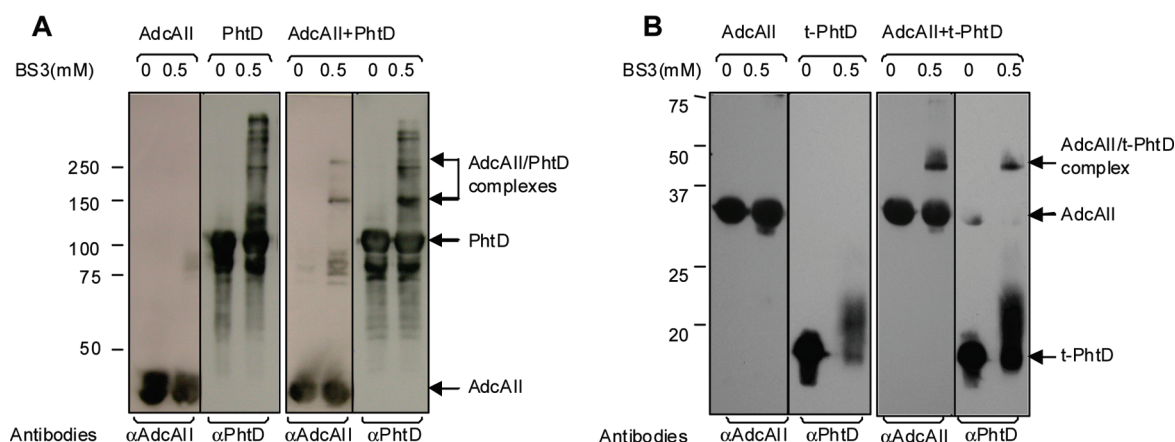
Figure 4. In vitro cross-linking of AdcAII and PhtD. The mixture of AdcAII and PhtD (A) or the mixture of AdcAII and t-PhtD (B) in an 8:1 ratio was incubated with 0.5 mM BS3 before being loaded on a 12.5% SDS–PAGE gel and analyzed by Western blotting. The same membrane was used for both antibody revelations; stripping was performed after the first revelation. The presence of two to three bands for PhtD is due to proteolytic cleavage of the protein under the experimental conditions.

metabolic pathway and interacted with each other. This putative interaction was tested by in vitro cross-linking experiments followed by Western blotting detection. As a control, each individual protein was incubated with the cross-linking agent. Cross-linking of the individual proteins showed that AdcAII remains mainly monomeric with a small amount of multimers with molecular masses between 75 and 100 kDa. Full-length PhtD generated a larger amount of high-molecular mass multimers (Figure 4A). The same pattern was observed regardless of the BS3 concentration used, from 0.1 to 1 mM (data not shown). When a mixture of both proteins was incubated with the cross-linking agent, two additional bands reacting with anti-AdcAII and anti-PhtD antibodies appeared with apparent molecular masses of 140 ± 5 and 245 ± 5 kDa, respectively (Figure 4A). These apparent masses are in agreement with the existence of AdcAII–PhtD complexes in the monomeric and dimeric form whose theoretical masses are 124 and 248 kDa, respectively. To map the region of PhtD involved in the interaction with AdcAII, we performed similar cross-linking experiments using t-PhtD. As shown in Figure 4B, when AdcAII and t-PhtD were mixed, a 47 kDa band reacting with both antibodies that did not occur with the isolated proteins was formed. This observation suggests that the first 30–167 amino acids of PhtD are sufficient to allow the formation of a 1:1 AdcAII–t-PhtD complex (theoretical molecular mass of 48 kDa).

AdcAII and PhtD Expression Is Corepressed by Zn^{2+}. Two adjacent palindromic sequences upstream of *adcAII* and *phtD* genes have previously been identified.[10] These sequences bind AdcR, a Zn^{2+}-dependent transcriptional repressor (Figure 1A). Very recently, it has been shown that PhtD mRNA expression is repressed by Zn^{2+}.[21] Thus, we assumed that expression of AdcAII and PhtD would be coregulated by Zn^{2+}, and to confirm this, we investigated the effects of Zn^{2+} on the expression of both genes. The *S. pneumoniae* R6 strain was cultured in a chemically defined medium (CDM) with or without supplementation with Zn^{2+} and transcription of *adcAII*, *phtD*, and *ccdA* (a gene upstream of the operon) quantified by real-time PCR. In the presence of 33 μM Zn^{2+}, the level of expression of both *adcAII* and *phtD* genes was reduced by ∼50% compared to that of the unsupplemented medium, while the level of transcription of the *ccdA* gene was not modified (Figure 5A). This correlated with a marked reduction
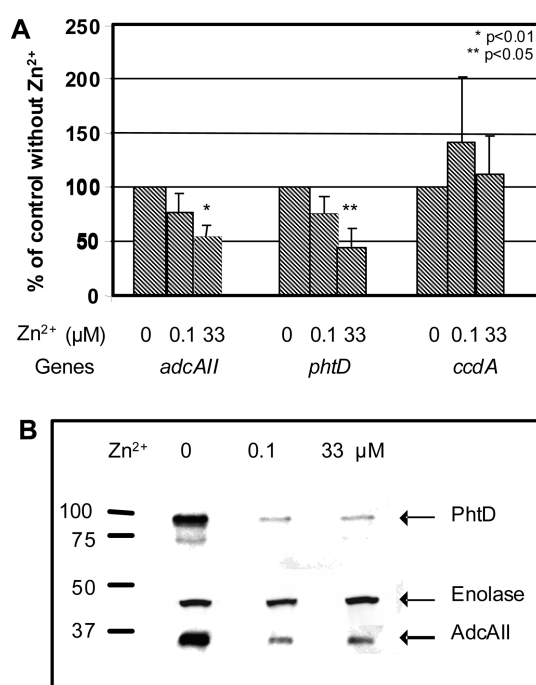
Figure 5. Zn^{2+} regulation of AdcAII and PhtD expression in *S. pneumoniae*. (A) Quantitative PCR was performed on RNA extracts of pneumococcus grown in CDM containing 0, 0.1, or 33 μM ZnCl$_2$. Copy numbers were reported to the *rpoB* internal control measured under the same conditions and expressed as a percentage of the amount from the culture without Zn^{2+}. Each cDNA from RNA extracts from one experiment was quantified twice. Values are the means of four independent pneumococcal cultures. (B) Western blot analysis of proteins expressed from the same cultures as in panel A. Equal amounts of total bacterial homogenates were loaded on a 12.5% SDS–PAGE gel. Polyclonal antibodies against AdcAII, PhtD, and enolase were used to reveal the expression level of each protein. This blot is representative of four independent experiments. Annotations marked on the left correspond to molecular masses (kilodaltons).

in AdcAII and PhtD protein levels from the same bacterial cultures (66 and 70% reductions, respectively) (Figure 5B). As expected, the expression of the housekeeping enolase remained stable at all Zn^{2+} concentrations used. A Zn^{2+} concentration of 0.1 μM was
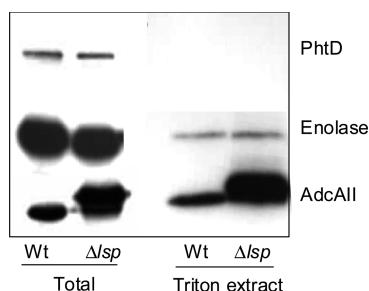
Figure 6. Lipoprotein identification. Western blot analysis of AdcAII and PhtD proteins expressed in WT and Δ*lsp* D39 strains. Equal amounts of total or phospholipid-associated proteins (Triton extract) were loaded on a 10% or 15% SDS−PAGE gel. Polyclonal antibodies against AdcAII, PhtD, and enolase were used to reveal the expression level of each protein. Annotations marked on the left correspond to molecular masses (kilodaltons).

not statistically significantly different from a Zn^{2+} concentration of 33 μM for the expression of *phtD* and *adcAII* at both gene and protein levels. In conclusion, Zn^{2+} represses transcription of the *adcAII* and *phtD* genes, leading to a reduction in the levels of protein expression, suggesting that both proteins may be involved in the metabolism of this metal.

AdcAII Is a Lipoprotein, and PhtD Is Not. The involvement of AdcAII and PhtD in the zinc metabolic pathway may occur at several levels. It may be related to the enzymatic activity of intracellular proteins, the transport of Zn^{2+}, or the ability of the bacterium to sense Zn^{2+} present in the host environment. Metal transport or extracellular metal sensing requires that at least one of the two proteins be expressed at the cell surface. To confirm the suggestion that AdcAII and PhtD are likely two pneumococcal lipoproteins,[22,23] we have performed computational analysis that has revealed the presence of the predicted LxxC lipobox in the sequence of each protein. However, further analysis failed to clearly recognize any positively charged amino acid patch in the initial residues of their sequence that do not allow their classification into the lipoprotein superfamily. Thus, to resolve the conflicting bioinformatic data, we used the previously described Δ*lsp* pneumococcus D39 mutant as a tool to identify whether AdcAII or PhtD is a lipoprotein.[15] The type II signal peptidase (Lsp) is responsible for the cleavage of the lipoprotein peptide signal after the covalent binding of lipoproteins to the membrane phospholipids via the conserved cysteine of the lipobox motif by the diacylglyceryl transferase (Lgt), leading to a mature lipoprotein with a slightly lower molecular mass. As shown in Figure 6, the molecular mass of the AdcAII protein in the total protein extract of the Δ*lsp* mutant was increased in comparison to that of the wild-type strain. Moreover, AdcAII protein is recovered from Triton extract that is specific for the lipoprotein fraction.[15] In contrast, the PhtD protein shows no molecular mass modification in the Δ*lsp* strain when compared to the wild type and was not detected in the Triton extract (Figure 6). Taken together, these data experimentally confirm that AdcAII is a lipoprotein and suggest that PhtD is not.

AdcAII and PhtD Are Localized at the Bacterial Surface. To further localize both proteins, we relied on subcellular fractionation and immunofluorescence experiments. Three pneumococcal fractions, including the cell wall, membranes, and the cytosol, were analyzed by Western blotting. AdcAII was detected exclusively in the membrane fraction, whereas PhtD was mainly recovered (84%) from the cell wall fraction (Figure 7A), supporting localization of both proteins at the cell surface. A minor fraction of the
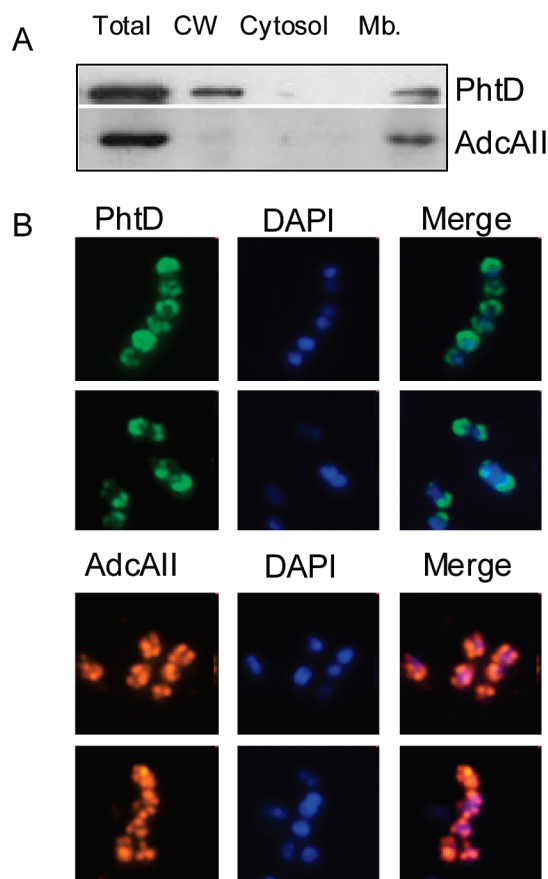
Figure 7. Localization of AdcAII and PhtD in *S. pneumoniae*. (A) Subcellular localization of AdcAII and PhtD. Equivalent amounts of each subcellular fraction, cell wall (CW), cytosol (Cytosol), and membrane (Mb.), were loaded onto a 12.5% SDS−PAGE gel and analyzed by immunoblotting using specific polyclonal antibodies revealed by chemiluminescence (ECL). (B) Immunofluorescence localization of AdcAII and PhtD. Bacteria grown to exponential phase (OD_{600} = 0.3) were deposited on slides, fixed, and incubated with primary antibodies directed against PhtD or AdcAII. Samples were then revealed with a secondary antibody coupled to Cy2 (PhtD) or Cy3 (AdcAII). The bacterial chromosome was stained with DAPI.

PhtD pool (16%) was present in the membrane fraction. The surface location of both proteins was confirmed by immunofluorescence experiments. *S. pneumoniae* cells were incubated with anti-PhtD and anti-AdcAII antibodies and labeled with Cy2- and Cy3-conjugated secondary IgG, respectively. As in Figure 7B, immunofluorescence analysis revealed that PhtD was mostly located at the poles of the bacterial cell surface whereas AdcAII appeared as foci located all over the periphery of the bacteria. Taken together, these data confirm the cell surface localization of AdcAII and PhtD, an essential prerequisite for their involvement in metal transport or extracellular metal sensing and zinc homeostasis.

■ **DISCUSSION**

In this work, we have demonstrated that PhtD specifically binds Zn^{2+} with a nanomolar affinity. This interaction stabilizes PhtD. We have established that PhtD and AdcAII are corepressed by Zn^{2+}. Furthermore, we have shown that the two molecules interact in vitro and are both located at the

pneumococcal surface with different immunofluorescence patterns and anchorage mechanisms.

Different computational and crystallographic data suggest that Pht proteins are able to bind to divalent ions. The presence of several histidine triad motifs in these proteins suggests that they are involved in Zn^{2+} binding.[10] The structure of a PhtA small fragment (amino acids 166—220) containing the second histidine triad repeat revealed a novel distorted tetrahedral coordination sphere for a Zn^{2+} ion composed of His194, His197, and His199 of the triad histidine motif and an additional asparagine (Asn173), which is unusual.[11,12] More recently, HtpA (a PhtD homologue from *S. pyogenes*) was purified using a Zn^{2+}-bound NTA column, indicating that HtpA is able to bind Zn^{2+}.[24] In this study, we confirm using a rigorous biochemical and biophysical analysis with complementary techniques (ICP-MS, TSA, and ITC) that PhtD is a Zn^{2+}-binding protein. As shown by the ICP-MS analysis, the full-length protein, which contains five histidine triads, includes five metallic atoms, which were identified as being mostly Zn^{2+}, with 10% of the metallic sites occupied by Ni^{2+}. This ion most probably replaced the native Zn^{2+} ion during the purification step on a Ni^{2+}-bound column. We confirmed zinc binding to PhtD by showing that the PhtD thermal stability is enhanced upon addition of Zn^{2+} but not upon addition of Mn^{2+}. Furthermore, the truncated protein t-PhtD (amino acids 30—167, encompassing a single histidine triad) exhibits one high-affinity Zn^{2+} binding site ($K_d = 131 \pm 10$ nM) using microcalorimetry titration techniques.

Both *adcAII* and *phtD* genes belong to an operon that includes one consensus AdcR-binding sequence followed by a second with a degenerate sequence. Both sites are located upstream of *adcAII*. *adcR* is part of the *adcABCR* operon that has been reported to be involved in the uptake of zinc.[6] AdcR has been shown to be a Zn^{2+}-dependent transcriptional repressor, the expression of which is regulated by environmental Zn^{2+} and Mn^{2+} concentrations.[25] Electrophoretic mobility shift assays of purified *Streptococcus suis* AdcR protein confirmed that the AdcR-binding sequence corresponds to the *in silico*-predicted motif (TTAACNRGTTAA) and that AdcR binding to its target palindromic sequence is dependent on the presence of either Zn^{2+} or Mn^{2+} in vitro.[26] AdcR is a homodimer in solution whose binding affinity for DNA is Zn^{2+}-stimulated with a K_{DNA-Zn} of 2.4×10^8 M^{-1}.[6] Previous publications have provided evidence that AdcR regulates *pht* gene repression in the D39 pneumoccocus,[6,27] and in a recent study, it was shown that Pht protein expression was downregulated by Zn^{2+} using flow cytometry analysis of pneumococcus incubated with antibodies against PhtE, PhtD/E, or PhtB/D proteins.[21] In our experiments, growing bacteria in chemically defined medium in which micromolar concentrations of Zn^{2+} has been added, corresponding to those encountered in the body,[2] we have shown Zn^{2+}-dependent repression not only of *phtD* but also of *adcAII*. On the basis of the data discussed above, we suggest that this repression is mediated by the Zn^{2+}-dependent repressor AdcR in a fashion similar to the one reported for PhtD.[6]

The mechanism by which AdcAII participates in the homeostasis of Zn^{2+} remains unclear. In this work, we have shown AdcAII is a lipoprotein. The crystal structure of AdcAII identified one tetrahedral Zn^{2+}-binding site,[3] suggesting that AdcAII might be the substrate binding component of a Zn^{2+} uptake ABC transporter. This would be reminiscent of the organization suggested for the homologous *S. pyogenes* laminin-binding protein Lsp (or Lbp).[4,5] AdcAII does not display the conventional ABC transporter genetic organization, and the putative corresponding ABC transporter permease and ATPase have not yet

been identified. Our data demonstrate that full-length PhtD binds five Zn^{2+} atoms per molecule and is localized mainly on the pneumococcal cell wall at the poles of bacteria grown to exponential phase in rich medium. We have also now provided evidence of a physical interaction between AdcAII and PhtD in vitro and evidence of the fact that they are cotranscribed. These data are compatible with a role for PhtD as an extracellular Zn^{2+} scavenger acting as a siderophore for acquisition of zinc by pneumococcus. The protein might convey the captured Zn^{2+} to the putative AdcAII transporter. Alternatively, the AdcAII—PhtD complex may be part of an environmental Zn^{2+} sensor linked to virulence. Other members of the Zn^{2+}-binding Pht family mediate the immune response[24,13] and the interaction with the host.[27] The latter work describes an interaction between the four Pht proteins of the D39 pneumococcus strain and the host H factor. This observation may be strain-dependent.[28] Our biochemical data support a critical role of the AdcAII—PhtD system in *S. pneumoniae* zinc homeostasis, a function that may be related to its virulence.

■ AUTHOR INFORMATION

Corresponding Author

*Institut de Biologie Structurale Jean-Pierre Ebel, 41 Rue Jules Horowitz, 38027 Grenoble cedex 1, France. Phone: 33-(0)4 38 78 96 81. Fax: 33-(0)4 38 78 54 94. E-mail: vernet@ibs.fr.

■ ABBREVIATIONS

ABC, ATP-binding cassette; ACES, *N*-(2-acetamido)-2-aminoethanesulfonic acid; CDM, chemically defined medium; DAPI, 6-diaminido-2-phenylindole; ICP-MS, inductively coupled plasma mass spectroscopy; ITC, isothermal titration calorimetry; MBR, metal-binding receptor; OD, optical density; TH broth, Bacto Todd Hewitt broth; T_m, melting temperature; TEV, tobacco etch virus; TSA, thermal shift assay.

■ REFERENCES

(1) Magneson, G. R., Puvathingal, J. M., and Ray, W. J., Jr. (1987) The concentrations of free Mg^{2+} and free Zn^{2+} in equine blood plasma. *J. Biol. Chem. 262*, 11140–11148.

(2) Zalewski, P. D., Truong-Tran, A. Q., Grosser, D., Jayaram, L., Murgia, C., and Ruffin, R. E. (2005) Zinc metabolism in airway epithelium and airway inflammation: Basic mechanisms and clinical targets. A review. *Pharmacol. Ther. 105*, 127–149.

(3) Loisel, E., Jacquamet, L., Serre, L., Bauvois, C., Ferrer, J. L., Vernet, T., Di Guilmi, A. M., and Durmort, C. (2008) AdcAII, a new pneumococcal Zn-binding protein homologous with ABC transporters: Biochemical and structural analysis. *J. Mol. Biol. 381*, 594–606.

(4) Linke, C., Caradoc-Davies, T. T., Young, P. G., Proft, T., and Baker, E. N. (2009) The laminin-binding protein Lbp from *Streptococcus pyogenes* is a zinc-receptor. *J. Bacteriol. 191*, 5814–5823.

(5) Weston, B. F., Brenot, A., and Caparon, M. G. (2009) The Metal Homeostasis Protein Lsp of *Streptococcus pyogenes* is Necessary for Acquisition of Zinc and Virulence. *Infect. Immun. 77*, 2840–2848.

(6) Reyes-Caballero, H., Guerra, A. J., Jacobsen, F. E., Kazmierczak, K. M., Cowart, D., Koppolu, U. M., Scott, R. A., Winkler, M. E., and Giedroc, D. P. (2010) The metalloregulatory zinc site in *Streptococcus pneumoniae* AdcR, a zinc-activated MarR family repressor. *J. Mol. Biol. 403*, 197–216.

(7) Adamou, J. E., Heinrichs, J. H., Erwin, A. L., Walsh, W., Gayle, T., Dormitzer, M., Dagan, R., Brewah, Y. A., Barren, P., Lathigra, R., Langermann, S., Koenig, S., and Johnson, S. (2001) Identification and characterization of a novel family of pneumococcal proteins that are protective against sepsis. *Infect. Immun. 69*, 949–958.

(8) Hamel, J., Charland, N., Pineau, I., Ouellet, C., Rioux, S., Martin, D., and Brodeur, B. R. (2004) Prevention of pneumococcal disease in mice immunized with conserved surface-accessible proteins. *Infect. Immun. 72*, 2659–2670.

(9) Wizemann, T. M., Heinrichs, J. H., Adamou, J. E., Erwin, A. L., Kunsch, C., Choi, G. H., Barash, S. C., Rosen, C. A., Masure, H. R., Tuomanen, E., Gayle, A., Brewah, Y. A., Walsh, W., Barren, P., Lathigra, R., Hanson, M., Langermann, S., Johnson, S., and Koenig, S. (2001) Use of a whole genome approach to identify vaccine molecules affording protection against *Streptococcus pneumoniae* infection. *Infect. Immun. 69*, 1593–1598.

(10) Panina, E. M., Mironov, A. A., and Gelfand, M. S. (2003) Comparative genomics of bacterial zinc regulons: Enhanced ion transport, pathogenesis, and rearrangement of ribosomal proteins. *Proc. Natl. Acad. Sci. U.S.A. 100*, 9912–9917.

(11) Riboldi-Tunnicliffe, A., Bent, C. J., Isaacs, N. W., and Mitchell, T. J. (2004) Expression, purification and X-ray characterization of residues 18−230 from the pneumococcal histidine triad protein A (PhtA) from *Streptococcus pneumoniae*. *Acta Crystallogr. D60*, 926–928.

(12) Riboldi-Tunnicliffe, A., Isaacs, N. W., and Mitchell, T. J. (2005) 1.2 Angstroms crystal structure of the *S. pneumoniae* PhtA histidine triad domain, a novel zinc binding fold. *FEBS Lett. 579*, 5353–5360.

(13) Godfroid, F., Hermand, P., Verlant, V., Denoel, P., and Poolman, J. T. (2011) Preclinical evaluation of the pht proteins as potential cross-protective pneumococcal vaccine antigens. *Infect. Immun. 79*, 238–245.

(14) van de Rijn, I., and Kessler, R. E. (1980) Growth characteristics of group A streptococci in a new chemically defined medium. *Infect. Immun. 27*, 444–448.

(15) Khandavilli, S., Homer, K. A., Yuste, J., Basavanna, S., Mitchell, T., and Brown, J. S. (2008) Maturation of *Streptococcus pneumoniae* lipoproteins by a type II signal peptidase is required for ABC transporter function and full virulence. *Mol. Microbiol. 67*, 541–557.

(16) Attali, C., Frolet, C., Durmort, C., Offant, J., Vernet, T., and Di Guilmi, A. M. (2008) *Streptococcus pneumoniae* choline-binding protein E interaction with plasminogen/plasmin stimulates migration across the extracellular matrix. *Infect. Immun. 76*, 466–476.

(17) Bordier, C. (1981) Phase separation of integral membrane proteins in Triton X-114 solution. *J. Biol. Chem. 256*, 1604–1607.

(18) Cockayne, A., Hill, P. J., Powell, N. B., Bishop, K., Sims, C., and Williams, P. (1998) Molecular cloning of a 32-kilodalton lipoprotein component of a novel iron-regulated *Staphylococcus epidermidis* ABC transporter. *Infect. Immun. 66*, 3767–3774.

(19) Harry, E. J., Pogliano, K., and Losick, R. (1995) Use of immunofluorescence to visualize cell-specific gene expression during sporulation in *Bacillus subtilis*. *J. Bacteriol. 177*, 3386–3393.

(20) Blasie, C. A., and Berg, J. M. (2002) Structure-based thermodynamic analysis of a coupled metal binding-protein folding reaction involving a zinc finger peptide. *Biochemistry 41*, 15068–15073.

(21) Rioux, S., Neyt, C., Di Paolo, E., Turpin, L., Charland, N., Labbe, S., Mortier, M. C., Mitchell, T. J., Feron, C., Martin, D., and Poolman, J. T. (2011) Transcriptional regulation, occurrence and putative role of the Pht Family of *Streptococcus pneumoniae*. *Microbiology 157*, 336–348.

(22) Hoskins, J., Alborn, W. E., Jr., Arnold, J., Blaszczak, L. C., Burgett, S., DeHoff, B. S., Estrem, S. T., Fritz, L., Fu, D. J., Fuller, W., Geringer, C., Gilmour, R., Glass, J. S., Khoja, H., Kraft, A. R., Lagace, R. E., LeBlanc, D. J., Lee, L. N., Lefkowitz, E. J., Lu, J., Matsushima, P., McAhren, S. M., McHenney, M., McLeaster, K., Mundy, C. W., Nicas, T. I., Norris, F. H., O'Gara, M., Peery, R. B., Robertson, G. T., Rockey, P., Sun, P. M., Winkler, M. E., Yang, Y., Young-Bellido, M., Zhao, G., Zook, C. A., Baltz, R. H., Jaskunas, S. R., Rosteck, P. R., Jr., Skatrud, P. L., and Glass, J. I. (2001) Genome of the bacterium *Streptococcus pneumoniae* strain R6. *J. Bacteriol. 183*, 5709–5717.

(23) Tettelin, H., Nelson, K. E., Paulsen, I. T., Eisen, J. A., Read, T. D., Peterson, S., Heidelberg, J., DeBoy, R. T., Haft, D. H., Dodson, R. J., Durkin, A. S., Gwinn, M., Kolonay, J. F., Nelson, W. C., Peterson, J. D., Umayam, L. A., White, O., Salzberg, S. L., Lewis, M. R., Radune, D., Holtzapple, E., Khouri, H., Wolf, A. M., Utterback, T. R., Hansen, C. L., McDonald, L. A., Feldblyum, T. V., Angiuoli, S., Dickinson, T., Hickey, E. K., Holt, I. E., Loftus, B. J., Yang, F., Smith, H. O., Venter, J. C., Dougherty, B. A., Morrison, D. A., Hollingshead, S. K., and Fraser, C. M. (2001) Complete genome sequence of a virulent isolate of *Streptococcus pneumoniae*. *Science 293*, 498–506.

(24) Kunitomo, E., Terao, Y., Okamoto, S., Rikimaru, T., Hamada, S., and Kawabata, S. (2008) Molecular and biological characterization of histidine triad protein in group A streptococci. *Microbes Infect. 10*, 414–423.

(25) Loo, C. Y., Mitrakul, K., Voss, I. B., Hughes, C. V., and Ganeshkumar, N. (2003) Involvement of the adc operon and manganese homeostasis in *Streptococcus gordonii* biofilm formation. *J. Bacteriol. 185*, 2887–2900.

(26) Aranda, J., Garrido, M. E., Fittipaldi, N., Cortes, P., Llagostera, M., Gottschalk, M., and Barbe, J. (2009) Protective capacities of cell surface-associated proteins of *Streptococcus suis* mutants deficient in divalent cation-uptake regulators. *Microbiology 155*, 1580–1587.

(27) Ogunniyi, A. D., Grabowicz, M., Mahdi, L. K., Cook, J., Gordon, D. L., Sadlon, T. A., and Paton, J. C. (2009) Pneumococcal histidine triad proteins are regulated by the Zn^{2+}-dependent repressor AdcR and inhibit complement deposition through the recruitment of complement factor H. *FASEB J. 23*, 731–738.

(28) Melin, M., Di Paolo, E., Tikkanen, L., Jarva, H., Neyt, C., Kayhty, H., Meri, S., Poolman, J., and Vakevainen, M. (2010) Interaction of pneumococcal histidine triad proteins with human complement. *Infect. Immun. 78*, 2089–2098.